

# Crystal Structure of the ATPase Subunit and Its Substrate-Dependent Association with the GATase Subunit: A Novel Regulatory Mechanism for a Two-Subunit-Type GMP Synthetase from *Pyrococcus horikoshii* OT3

Shintaro Maruoka, Shoichiro Horita, Woo Cheol Lee, Koji Nagata and Masaru Tanokura\*

Department of Applied Biological Chemistry, Graduate School of Agricultural and Life Sciences, University of Tokyo, 1-1-1 Yayoi, Bunkyo-ku, Tokyo 113-8657, Japan

Received 9 July 2009;  
received in revised form  
17 October 2009;  
accepted 23 October 2009  
Available online  
10 November 2009

Guanosine 5'-monophosphate synthetase(s) (GMPS) catalyzes the final step of the *de novo* synthetic pathway of purine nucleotides. GMPS consists of two functional units that are present as domains or subunits: glutamine amidotransferase (GATase) and ATP pyrophosphatase (ATPPase). GATase hydrolyzes glutamine to yield glutamate and ammonia, while ATPase utilizes ammonia to convert adenylyl xanthosine 5'-monophosphate (adenyl-XMP) into guanosine 5'-monophosphate. Here we report the crystal structure of PH-ATPPase (the ATPase subunit of the two-subunit-type GMPS from the hyperthermophilic archaeon *Pyrococcus horikoshii* OT3). PH-ATPPase consists of two domains (N-domain and C-domain) and exists as a homodimer in the crystal and in solution. The N-domain contains an ATP-binding platform called P-loop, whereas the C-domain contains the xanthosine 5'-monophosphate (XMP)-binding site and also contributes to homodimerization. We have also demonstrated that PH-GATase (the glutamine amidotransferase subunit of the two-subunit-type GMPS from the hyperthermophilic archaeon *P. horikoshii* OT3) alone is inactive, and that all substrates of PH-ATPPase except for ammonia ( $Mg^{2+}$ , ATP and XMP) are required to stabilize the active complex of PH-ATPPase and PH-GATase subunits.

© 2009 Elsevier Ltd. All rights reserved.

Edited by G. Schulz

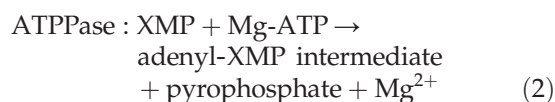
**Keywords:** ATP pyrophosphatase; crystal structure; glutamine amidotransferase; GMPS; purine nucleotide biosynthesis

## Introduction

Guanosine 5'-monophosphate synthetase(s) (GMPS) is a widespread enzyme seen in all domains of life. GMPS is required for the final step of the *de novo* synthesis of guanine nucleotides, converting xanthosine 5'-monophosphate (XMP) into guano-

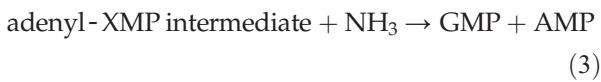
sine 5'-monophosphate (GMP), a precursor of DNA and RNA. GMPS is also involved in chromatin regulation<sup>1</sup> and axon guidance,<sup>2</sup> as shown in *Drosophila*. In addition, GMPS has been studied as an important chemotherapeutic target for immunosuppressive agents.<sup>3</sup>

GMPS belongs to the class I glutamine amidotransferase (GATase) family and consists of two catalytic units, GATase and ATP pyrophosphatase (ATPPase):



\*Corresponding author. E-mail address: [amtanok@mail.ecc.u-tokyo.ac.jp](mailto:amtanok@mail.ecc.u-tokyo.ac.jp).

Abbreviations used: GMPS, guanosine 5'-monophosphate synthetase(s); GATase, glutamine amidotransferase; ATPase, ATP pyrophosphatase; XMP, xanthosine 5'-monophosphate; GMP, guanosine 5'-monophosphate; PDB, Protein Data Bank; GDH, glutamate dehydrogenase; EDTA, ethylenediaminetetraacetic acid; adenylyl-XMP, adenylyl xanthosine 5'-monophosphate.



GATase hydrolyzes glutamine to generate glutamate and ammonia (Reaction (1)), and ATPase adenylates XMP to form an adenylyl xanthosine 5'-monophosphate (adenyl-XMP) intermediate in the presence of  $\text{Mg}^{2+}$ , ATP, and XMP (Reaction (2)). The highly reactive adenylyl-XMP intermediate is then aminated by ammonia provided by GATase (Reaction (3)).<sup>4-6</sup> Overall, GMP is generated by the concerted reactions of these two catalytic units.<sup>7,8</sup>

The two catalytic units are either encoded by a single gene (two-domain type) in eukaryotes, bacteria, and some archaea, or encoded by two separate genes (two-subunit type) in other archaea. In two-domain-type GMPS, the GATase domain is located in the N-terminal half, and the ATPase domain is located in the C-terminal half; in two-subunit-type GMPS, these two units exist as separate polypeptides (Fig. 1a). Almost all structural and functional studies on GMPS have been carried out for two-domain-type GMPS from humans,<sup>11-13</sup> rats,<sup>14</sup> mice,<sup>15</sup> *Escherichia coli*,<sup>6,16-19</sup> and *Plasmodium falciparum*.<sup>20</sup> So far, the crystal structures of three two-domain-type GMPS—EC-GMPS (the two-domain-type GMPS from *E. coli*) [Protein Data Bank (PDB) ID 1GPM],<sup>21</sup> TT-GMPS (the two-domain-type GMPS from *Thermus thermophilus*) (PDB IDs 2YWB and 2YWC; Baba *et al.*, unpublished results), and HS-GMPS (the two-domain-type GMPS from *Homo sapiens*) (PDB ID 2VXO; Welin *et al.*, unpublished results)—and two two-subunit-type GMPS—the GATase subunit from *Thermoplasma acidophilum* (PDB ID 2A9V; Joint Center for Structural Genomics, unpublished results)

and *Pyrococcus horikoshii* (PDB ID 1WL8; Lokanath and Kunishima, unpublished results) (PDB ID 2D7J; Maruoka *et al.*<sup>22</sup>), and the ATPase subunit from *P. horikoshii* (PDB ID 2DPL; Asada and Kunishima, unpublished results) (PDB ID 3A4I; this study)—have been deposited in the PDB. In the crystal structures of two-domain-type GMPS, the two active sites of the GATase and ATPase domains are exposed to the solvent, and it has not been revealed yet how the putative ammonia channel, which efficiently couples the GATase and ATPase reactions, is formed.<sup>21</sup>

To gain insights into the catalytic and regulatory mechanisms of GMPS, particularly two-subunit-type GMPS, we have determined the crystal structures of the GATase subunit [PH-GATase (the glutamine amidotransferase subunit of the two-subunit-type GMPS from the hyperthermophilic archaeon *P. horikoshii* OT3); PDB ID 2D7J]<sup>22</sup> and the ATPase subunit [PH-ATPase (the ATPase subunit of the two-subunit-type GMPS from the hyperthermophilic archaeon *P. horikoshii* OT3); this study] of PH-GMPS (the two-subunit-type GMPS from the hyperthermophilic archaeon *P. horikoshii* OT3) and analyzed the regulatory mechanisms of PH-GMPS. Our crystal structure has revealed that the ATPase subunit of PH-GMPS (PH-ATPase) is very similar to the ATPase domains of EC-GMPS and TT-GMPS in terms of backbone fold, ATP-binding and XMP-binding residues, and dimerization mode, but is dissimilar with respect to the relative orientation of N-domain and C-domain. PH-ATPase is also similar to the ATPase domain of HS-GMPS in terms of backbone fold and ligand-binding residues, but is dissimilar in oligomerization mode because HS-GMPS exists as a monomer in solution.<sup>12</sup> We also performed activity assays

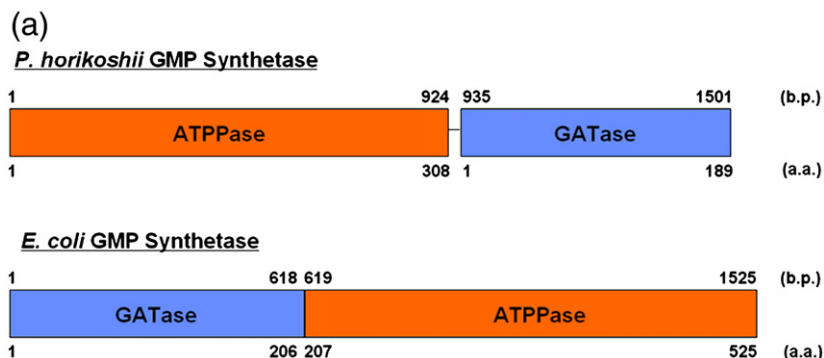


**Fig. 1.** (a) Gene and protein structure of GMPS from *P. horikoshii* and *E. coli*. *P. horikoshii* GMPS is encoded by two genes, *ph1346* (encoding GATase) and *ph1347* (encoding ATPase), located 7 bp apart. *E. coli* GMPS is encoded by a single gene *guaA*, which encodes the GATase domain in the N-terminal half and the ATPase domain in the C-terminal half. (b) Multiple sequence alignment of ATPase subunits and domains. The proteins are derived from *P. horikoshii*, *T. thermophilus*, and *E. coli*. The secondary structure elements of PH-ATPase are shown above the alignment. Sequence alignment was obtained with CLUSTAL W.<sup>9</sup> The figure was prepared with ESPript.<sup>10</sup>  $\alpha$ -Helices,  $3_{10}$ -helices, and  $\beta$ -strands are denoted as  $\alpha$ ,  $\eta$ , and  $\beta$ , respectively. Completely and highly conserved residues are boxed and indicated by white letters on a red background and red letters on a white background, respectively. Blue and green triangles indicate the putative binding residues for ATP and XMP, respectively. Red triangles indicate residues forming intermolecular hydrogen bonds in homodimers of PH-ATPase, EC-GMPS, and TT-GMPS.



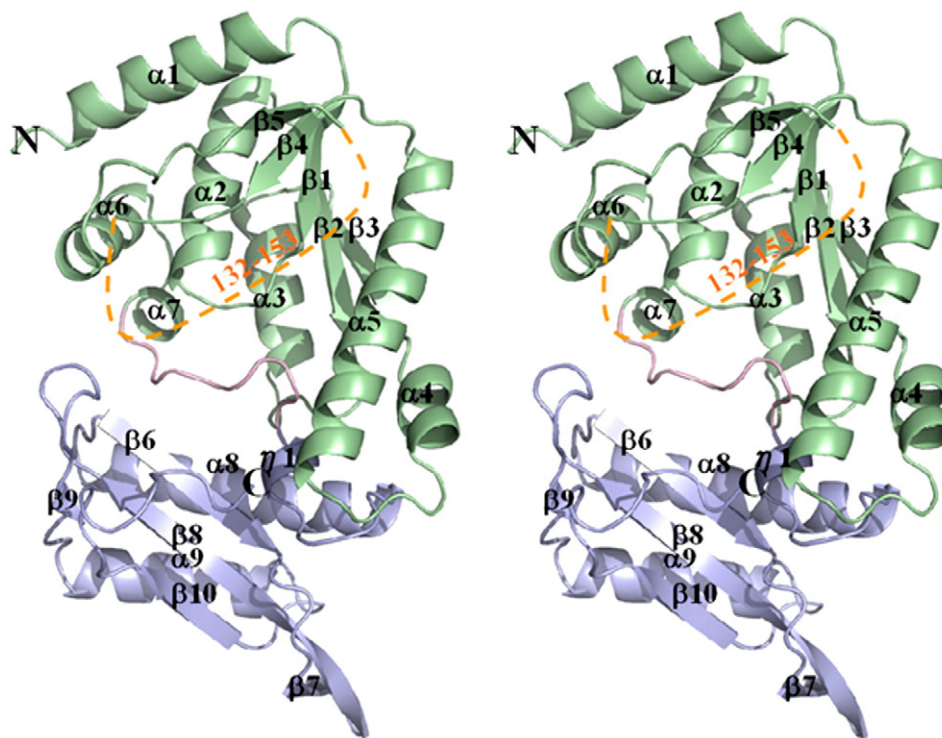


**Fig. 2.** Stereoview of the PH-ATPPase protomer (molecule A). The termini and secondary structures are labeled. N-domains and C-domains are shown in green and blue, respectively. The Pro-rich interdomain loop is shown in pink. The 22-residue disordered peptide is depicted with an orange dotted line. The figure was generated using the program PyMOL.

and  $R_{\text{free}}$  values of 21.0% and 24.6%, respectively. There are two protomers (referred to as chains A and B) of PH-ATPPase that form a homodimer in the asymmetric unit (Fig. 3a). The final model of PH-ATPPase consists of residues 1–131 and 154–308 (286 of 308 residues, covering 92.9% of the sequence) for both chains A and B. No electron densities are observed for the remaining residues. The Ramachandran plot shows that all the  $\varphi$ - $\psi$  pairs lie in the most favored and additionally allowed regions (Table 1). The two protomers in the PH-ATPPase homodimer are very similar to each other, as shown by the small root-mean-square deviation (RMSD) of 0.34 Å for 263 C $\alpha$  atom pairs. Major structural differences between them are caused by crystal contacts and are located in two regions: residues 240–248 and 261–263.

The protomer of PH-ATPPase consists of two domains: the N-domain (residues 1–186) and the C-domain (residues 187–308) (Fig. 2). The larger N-domain is composed of a five-stranded parallel  $\beta$ -sheet and  $\alpha$ -helical layers on both sides of the sheet. Electron densities are not observed for 22 continuous residues (residues 132–153) located between  $\beta$ 4 and  $\beta$ 5 (Fig. 2). The N-domain contains a glycine-rich ATP-binding motif called the “P-loop motif” (residues 28–34; SGGVDSS) located after  $\beta$ 1. This P-loop motif is strictly conserved in the ATPase subunits/domains of GMPS (Fig. 1b); thus, the N-domain is considered to be responsible for ATP binding. The C-domain, consisting of three  $\alpha$ -helices and five  $\beta$ -strands, serves as the dimerization

domain. The dimer interface is mainly formed by the  $\alpha$ 10 helix and a three-stranded parallel  $\beta$ -sheet consisting of  $\beta$ 7,  $\beta$ 8, and  $\beta$ 9.

In the dimer interface, approximately 11% (1500 Å<sup>2</sup>) of the surface area per protomer is buried, as indicated by the PISA server.<sup>23</sup> The gel-filtration chromatogram of PH-ATPPase indicates that the protein also behaves as a homodimer (ca 70 kDa) in solution (Fig. 7). The dimer interface contains 28 hydrogen bonds and eight salt bridges, which contribute to homodimerization. In particular, two *cis*-prolines (Pro301-Pro302) located after  $\beta$ 10 enable the formation of a tetrad of Asp296, Thr304, Glu306, and Arg292' (the prime denotes a residue from the other subunit) whose side chains contribute to homodimerization by electrostatic interactions. The residues Arg292, Val293, Tyr295, Asp296, and Thr304, which form intermolecular hydrogen bonds, are conserved in PH-ATPPase, TT-GMPS, and EC-GMPS (Fig. 4). These residues are also conserved in human GMPS (referred to as HS-GMPS), with the exception of Val293 (Ile in HS-GMPS), but they are not involved in dimerization in the crystal or in solution. HS-GMPS exists as a homodimer in the crystal (PDB ID 2VXO), but the mode of dimerization is different from those of PH-ATPPase, EC-GMPS, and TT-GMPS (Fig. 4). On the other hand, HS-GMPS exists as a monomer in solution, as shown by density gradient centrifugation.<sup>12</sup>

In addition to our crystal structure (PDB ID 3A4I), another crystal structure of PH-ATPPase at 1.43 Å resolution was deposited in the PDB (PDB ID 2DPL) by Asada *et al.* (unpublished results).

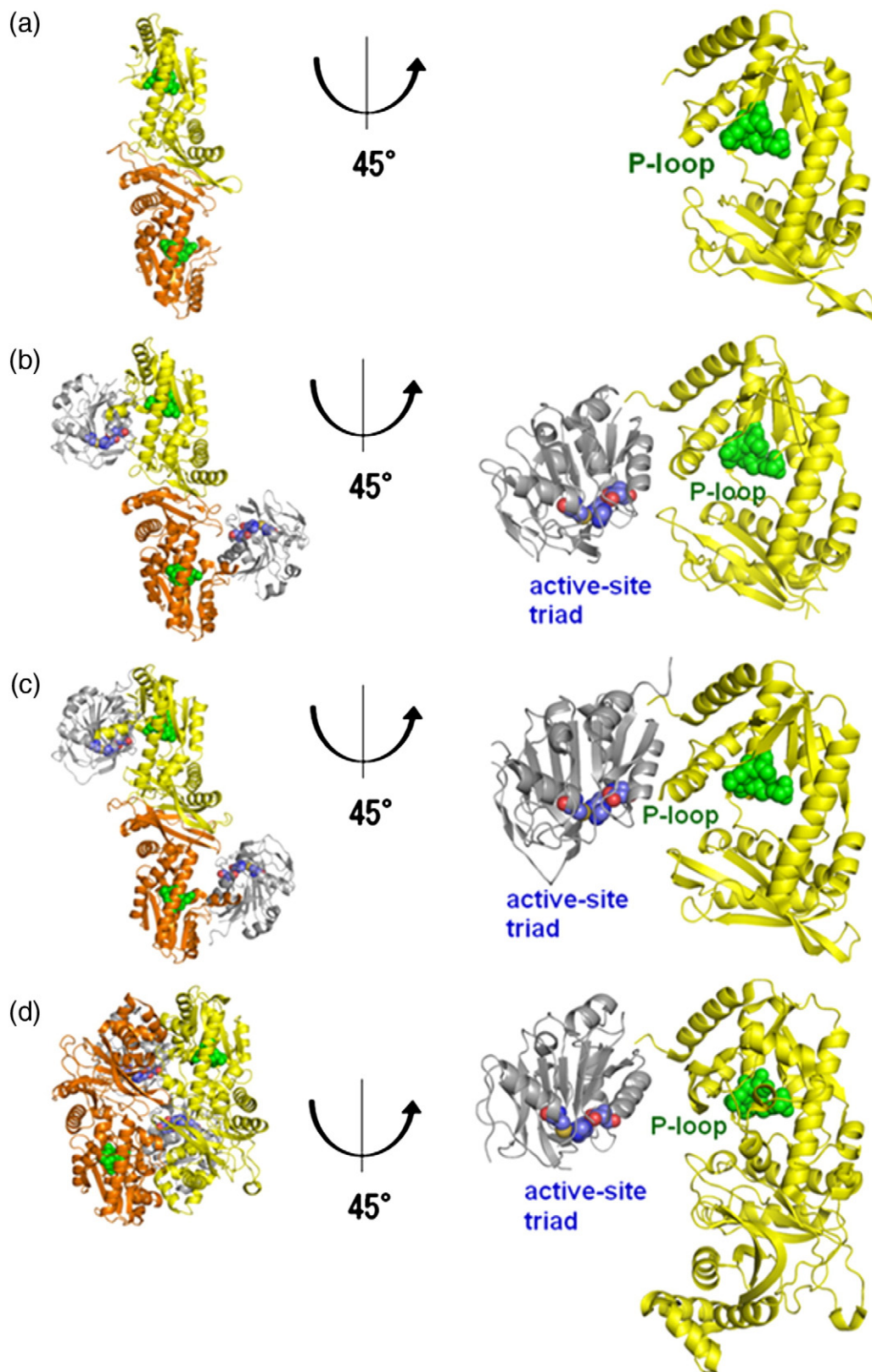


**Fig. 3.** The overall structure of the PH-ATPPase homodimer (a) compared to those of the TT-GMPS homodimer (b), the EC-GMPS homodimer (c), and the HS-GMPS homodimer (d). Each protomer is shown in yellow and orange. Each active-site triad of the GATase domain is shown with a blue sphere. The ATP-binding motif, called the “P-loop motif,” is indicated with a green sphere.

**Table 1.** Data collection and refinement statistics

<i>Data collection</i>	
Space group	$P2_12_12_1$
Unit cell parameters	
$a$ (Å)	69.9
$b$ (Å)	82.2
$c$ (Å)	111.6
Resolution <sup>a</sup> (Å)	50.0–1.79 (1.85–1.79)
Observed reflections	537,148
Unique reflections	60,634
Completeness <sup>a</sup> (%)	98.4 (100.0)
$R_{\text{merge}}^a$	0.052 (0.076)
$\langle I \rangle / \langle \sigma(I) \rangle^a$	28.1 (3.3)
<i>Refinement</i>	
Resolution range (Å)	50.0–1.79
$R_{\text{work}}$ (%)	21.0
$R_{\text{free}}$ (%)	24.6
Average $B$ -factors of protein	21.4
heavy atoms (Å <sup>2</sup> )	
Number of protein heavy atoms	4528
Number of water molecules	282
RMSD from ideal geometry	
Bond lengths (Å)	0.015
Bond angles (°)	1.361
Ramachandran plot	
Most favored region (%)	95.1
Additionally favored regions (%)	4.9

<sup>a</sup> The data of the highest-resolution shell are shown in parentheses.

The space group and unit cell dimensions of our crystals and those of Asada *et al.* are essentially the same: PDB ID 3A4I,  $P2_12_12_1$ ,  $a=69.9$  Å,  $b=82.2$  Å, and  $c=111.6$  Å; PDB ID 2DPL,  $P2_12_12_1$ ,  $a=70.4$  Å,  $b=83.3$  Å, and  $c=112.3$  Å. Moreover, our crystals and their crystals were obtained at very similar pH values, although the temperatures were different: PDB ID 3A4I at pH 8.4 and 278 K, and PDB ID 2DPL at pH 8.5 and 291 K. Since the two kinds of crystals obtained at very similar pH values belong to the same space group and have almost the same unit cell dimensions, the two crystal structures of PH-ATPPase are essentially the same, with a small RMSD of 0.446 Å for 564 C<sup>α</sup> atom pairs in the homodimer between PDB IDs 3A4I and 2DPL. We use our crystal structure (PDB ID 3A4I) for the following discussions.

### Structural comparison of PH-ATPPase with ATPase domains in two-domain-type GMPS

The structure of PH-ATPPase was compared with the reported structures of ATPase domains in the two-domain-type GMPS from *E. coli* (PDB ID 1GPM)<sup>21,24</sup> and *T. thermophilus* (PDB ID 2YWC; Baba *et al.*, unpublished results). PH-ATPPase is structurally similar to the corresponding domains of EC-GMPS and TT-GMPS (55% and 53% identical in sequence), with RMSDs of 1.04 Å and 1.24 Å (for 264 and 240 C<sup>α</sup> atom pairs), respectively. Remarkable differences, however, are observed in the relative orientation between the N-domain and the C-domain among these ATPase subunits/domains: a difference of 8° between PH-ATPPase and EC-

GMPS, and a difference of 5° between PH-ATPPase and TT-GMPS. This suggests the presence of a hinge motion between the N-domain and the C-domain (Fig. 5; Figs. S1 and S2, and Tables S1 and S2), as also suggested by the reaction mechanism of ATPase (described later in this section). The relative orientations of the N-domain and C-domain of PH-ATPPase are almost the same among the four chains of PDB IDs 3A4I and 2DPL (Table S3), suggesting that domain orientation would be most prevalent in unliganded PH-ATPPase, although the crystal packing effect cannot be denied.

Since the crystal structures of EC-GMPS (PDB ID 1GPM)<sup>21,24</sup> and TT-GMPS (PDB ID 2YWC) contained bound AMP and P<sub>i</sub><sup>21</sup> and bound XMP, respectively, the putative ATP-binding site and XMP-binding site of PH-ATPPase can be readily identified by superimposing the structures. The putative ATP-binding site is located in the N-domain, and all the putative ATP-recognizing amino acid residues (Fig. 6a) are conserved between PH-ATPPase and EC-GMPS, except for Ala26/Gly233 and Ile125/Ala333, whose main-chain atoms are involved in ATP recognition. Thus, PH-ATPPase would probably recognize ATP as EC-GMPS recognizes AMP and P<sub>i</sub> in the crystal structure. The purine base, ribose ring, and triphosphate of ATP would be recognized by Val53 and Phe108; Ala26-Leu27 and Ile125; and Ser28, Asp32-Ser33, Lys166, and Phe188, respectively. On the other hand, all residues of the putative XMP-binding site are located in the C-domain, except for Arg101, and all of the putative XMP-recognizing amino acid residues (Fig. 6b) are conserved between PH-ATPPase and TT-GMPS. Thus, PH-ATPPase would probably recognize XMP as does TT-GMPS. The purine base, ribose ring, and phosphate of XMP would be recognized by Arg101 and Pro189-Gly190-Pro-191; Gln229 and Glu306; and Lys300, Ile305-Gln306, and Glu308, respectively.

We have modeled bound ATP and XMP on the crystal structures of PH-ATPPase, EC-GMPS, and PH-GMPS. The two atoms P<sup>α</sup> of ATP and O<sup>2</sup> of XMP, which will form a covalent bond (1.5 Å) to yield the adenylyl-XMP intermediate,<sup>4</sup> are separated by 3.3 Å, 4.4 Å, and 5.5 Å in the crystal structures of TT-GMPS, PH-ATPPase, and EC-GMPS, respectively. These observations suggest that further movement between the N-domain and the C-domain has to occur for the reaction catalyzed by the ATPase subunits/domains to proceed.

### Substrate-induced stable complex formation of PH-ATPPase with PH-GATase

To examine the effects of the substrates of PH-ATPPase on the interaction between PH-GATase and PH-ATPPase, we performed gel-filtration chromatography with a Superdex 75 10/30 HR column (GE Healthcare) at room temperature (Fig. 7). The two subunits form a stable complex exclusively in the presence of 10 mM MgCl<sub>2</sub>, 0.1 mM ATP, and 0.1 mM XMP (buffer f). The stable complex

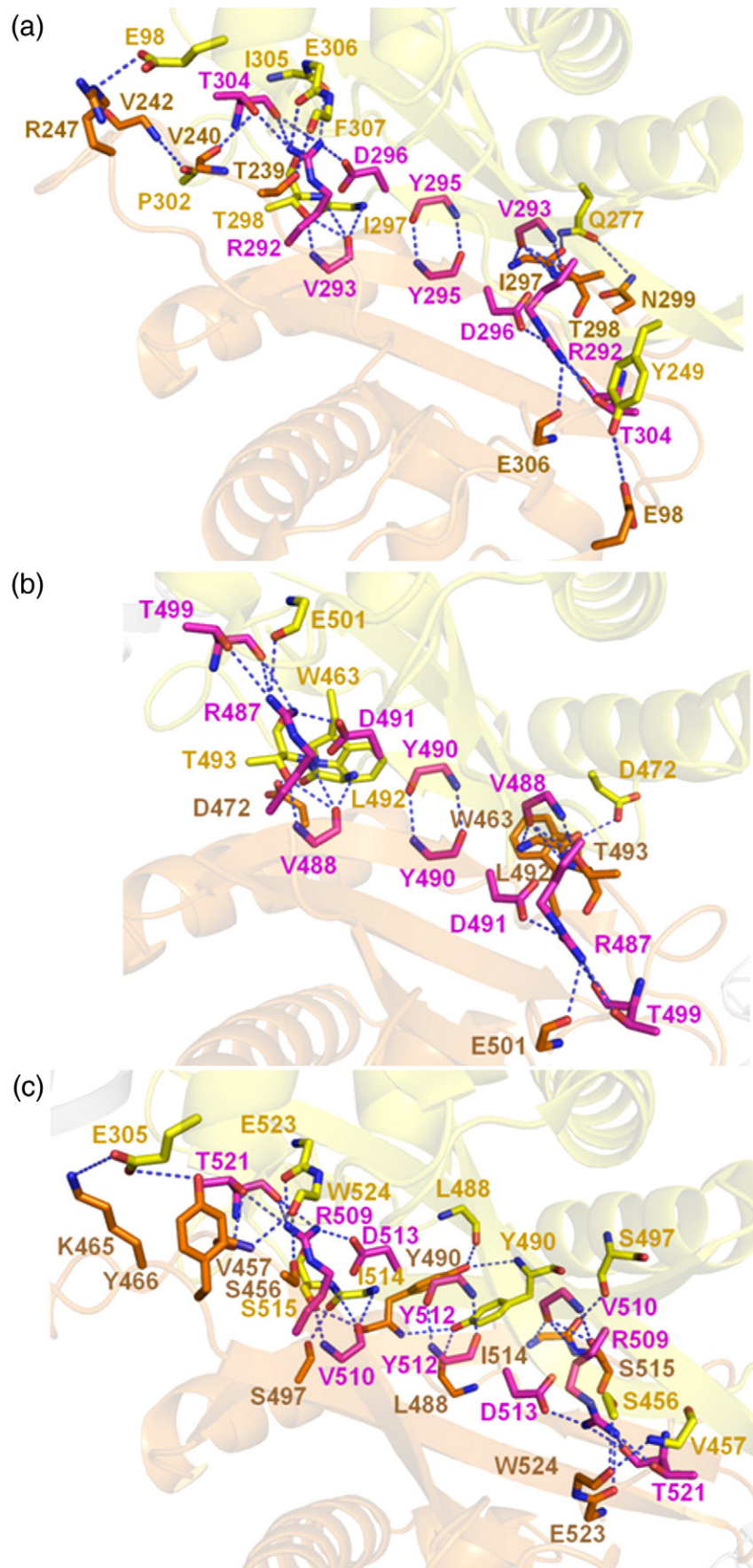
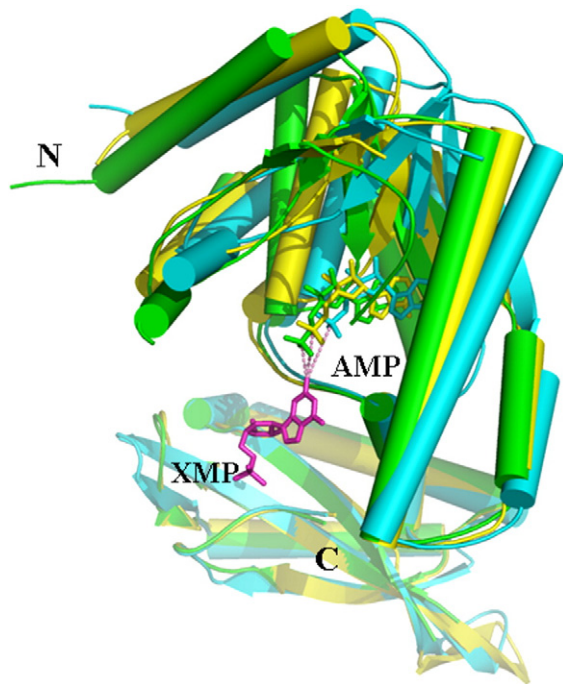


Fig. 4 (legend on next page)



**Fig. 5.** Structural comparisons of PH-ATPPase, EC-GMPS (PDB ID 1GPM), and TT-GMPS (PDB ID 2YWC). The C-terminal domain of PH-ATPPase is superimposed onto the C-terminal domain of EC-GMPS (cyan) complexed with AMP (cyan), and onto the C-terminal domain of TT-GMPS (green) complexed with XMP (magenta). The superimposed C-terminal domains are transparent to better visualize the bent conformations of the N-terminal domains.  $\alpha$ -Helices are depicted as cylinders, and  $\beta$ -strands are depicted as arrows. The AMPs bound to PH-ATPPase and TT-GMPS (depicted as yellow and green sticks, respectively) are modeled based on the superimposition of the N-terminal domains of the three proteins.

formation, however, is not observed when any one of the ATPase substrates is omitted from the buffer (buffers a–e). The results clearly show that all the substrates of PH-ATPPase except for ammonia ( $\text{Mg}^{2+}$ , ATP and XMP) are required for stabilizing the PH-GMPS complex formed by PH-GATase and PH-ATPPase subunits. The ATP cannot be replaced by AMP and  $\text{PPi}$  (buffer g). Since  $\text{Mg-ATP}$  and XMP are required to yield the adenylyl-XMP intermediate, these results suggest that the formation of the adenylyl-XMP intermediate would be important in stabilizing the PH-GMPS complex.

#### Effect of PH-GMPS complex formation on PH-GATase activity

To examine the effect of PH-GMPS complex formation on the activity of PH-GATase, we measured the glutaminase activity of PH-GATase

using a coupled assay with glutamate dehydrogenase (GDH) in the presence or in the absence of PH-ATPPase and its substrates, which are required for the complex formation ( $\text{Mg}^{2+}$ , ATP, and XMP) (Fig. 8a). The results revealed that PH-GATase alone does not show any measurable glutaminase activity (Condition (2)). PH-GATase is activated by the copresence of PH-ATPPase (Condition (4)). Moreover, the activity of PH-GATase is enhanced approximately fivefold by the copresence of PH-ATPPase and its substrates ( $\text{Mg}^{2+}$ , ATP, and XMP) (Condition (5)). Because these PH-ATPPase substrates show no direct effect on PH-GATase (Condition (3)), they are considered to enhance PH-GATase activity by stabilizing the PH-GMPS complex, as shown in Fig. 7. Assuming that PH-GMPS complex formation and PH-GATase activation are coupled, the results of the GATase activity assay suggest that the substrates of PH-ATPPase are not necessarily required for complex formation and that the PH-GMPS complex without all ATPase ligands would be unstable. Thus, PH-GATase consumes much less glutamine, unless all the components required for GMPS activity are present. This regulation mechanism is effective in avoiding glutamine wasting.

A similar phenomenon has been observed for EC-GMPS, a two-domain-type GMPS; that is, the GATase activity of EC-GMPS depends on the presence of the substrates for ATPase ( $\text{Mg}^{2+}$ , ATP, and XMP),<sup>25</sup> but the molecular mechanism for the substrate dependency of EC-GMPS remains unknown. Here we show that the substrates for ATPase promote the association of the GATase and ATPase subunits of PH-GMPS and also activate PH-GATase. Based on the high sequence similarity of these two subunits (50% identity), the same regulatory mechanism would likely be used in EC-GMPS.

#### Effect of ammonia on PH-ATPPase activity

To examine the effect of ammonia on the activity of PH-ATPPase, we measured ATPase activity (Fig. 8b). PH-ATPPase is capable of utilizing ammonia derived from ammonium chloride (Condition (2)), as well as ammonia derived from glutamine by PH-GATase in the manner of EC-GMPS (Condition (1)).<sup>26</sup> The copresence of ammonium chloride and glutamine does not promote ATPase activity additively, but decreases ATPase activity to a level similar to that observed in Condition (1) (Condition (3)). Thus, the glutamine-dependent and ammonium-chloride-dependent reactions are not independent. Interestingly, the ATPase activity increases approximately 1.5-fold when PH-GATase is omitted from the reaction mixture of Condition (3) (Condition (4)). This comparison (Conditions (3) and (4)) clearly

**Fig. 4.** The dimer interface of PH-ATPPase (a), TT-GMPS (b), and EC-GMPS (c). The amino acid residues involved in hydrogen bonds between protomers are represented by sticks and labeled. Hydrogen bonds are shown by dotted lines. The color scheme is the same as that in Fig. 3. (i) The dimer interface of PH-ATPPase. (ii) The dimer interface of TT-GMPS. (iii) The dimer interface of EC-GMPS. The conserved residues are shown in magenta.

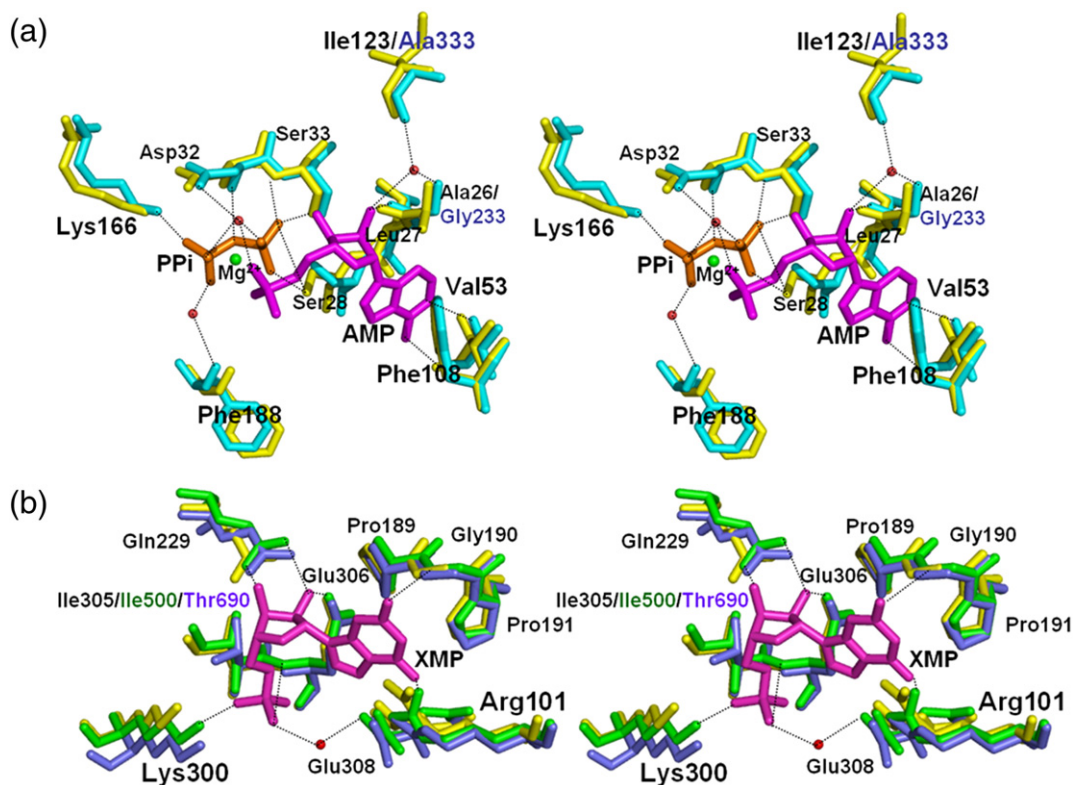


**Fig. 6.** Putative ligand recognition by PH-ATPPase. (a) Structural superposition of the ATP-binding site of PH-ATPPase (yellow) and *E. coli* GMPS (blue). AMP (magenta) and PPI (orange) from *E. coli* GMPS are also depicted with stick models. (b) Structural superposition of the XMP-binding site of PH-ATPPase (yellow) and *T. thermophilus* GMPS (blue). XMP (light magenta) from *T. thermophilus* GMPS is depicted with a stick model.

shows that the complex formation by PH-GATase and PH-ATPPase partly blocks the direct access of ammonium-chloride-derived ammonia to the active site of the PH-ATPPase and suggests the existence of an ammonia channel that prevents glutamine-derived ammonia from being released into the free ammonia pool prior to incorporation into XMP. Moreover, the results (Conditions (1), (2), and (3)) suggest that glutamine binding to GATase may complement the full shielding of the ammonia channel of the GMPS complex.

### Two-subunit-type GMPS and two-domain-type GMPS

To examine the distribution of the two-subunit-type and two-domain-type GMPS, we collected DNA sequence information for 565 GMPS in the three domains—41 in archaea, 482 in bacteria, and 42 in eukarya—from the KEGG database†. All GMPS from eukarya and bacteria are two-domain-type GMPS consisting of GATase and ATPase domains. In contrast, the GMPS from archaea include 6 two-domain-type GMPS and 34 two-subunit-type GMPS, indicating that two-subunit-type GMPS are unique and major properties of

archaea. The distribution of the two-subunit-type GMPS in archaea, however, is not correlated with the phylogenetic tree based on ribosomal proteins<sup>27</sup> because both two-domain-type GMPS and two-subunit-type GMPS are distributed in Euryarchaeota and Crenarchaeota. Two-subunit-type archaeal GMPS can be divided into two groups: one group in which the genes encoding GATase and ATPase subunits are colocalized (*Pyrococcus*, *Thermococcus*, *Methanobacterium*, *Methanobrevibacter*, and *Methanospaera*) and the other group in which the two genes are located apart. The separate GMPS genes may contribute to the compact genome size of many archaeal species by enabling the GATase subunit to be shared by various enzymes that utilize ammonia as substrate.

## Materials and Methods

### Expression and purification of PH-ATPPase for structure determination

The gene encoding PH-ATPPase (*ph1347*) was amplified by PCR using the genomic DNA of *P. horikoshii* OT3 as template. The PCR product was digested with NdeI and EcoRI, and ligated into the expression vector pET-26b(+) (Novagen). The *E. coli* strain Rosetta(DE3) (Novagen) was used as the host for protein expression. The cells were

† <http://www.kegg.jp/kegg/kegg2.html>

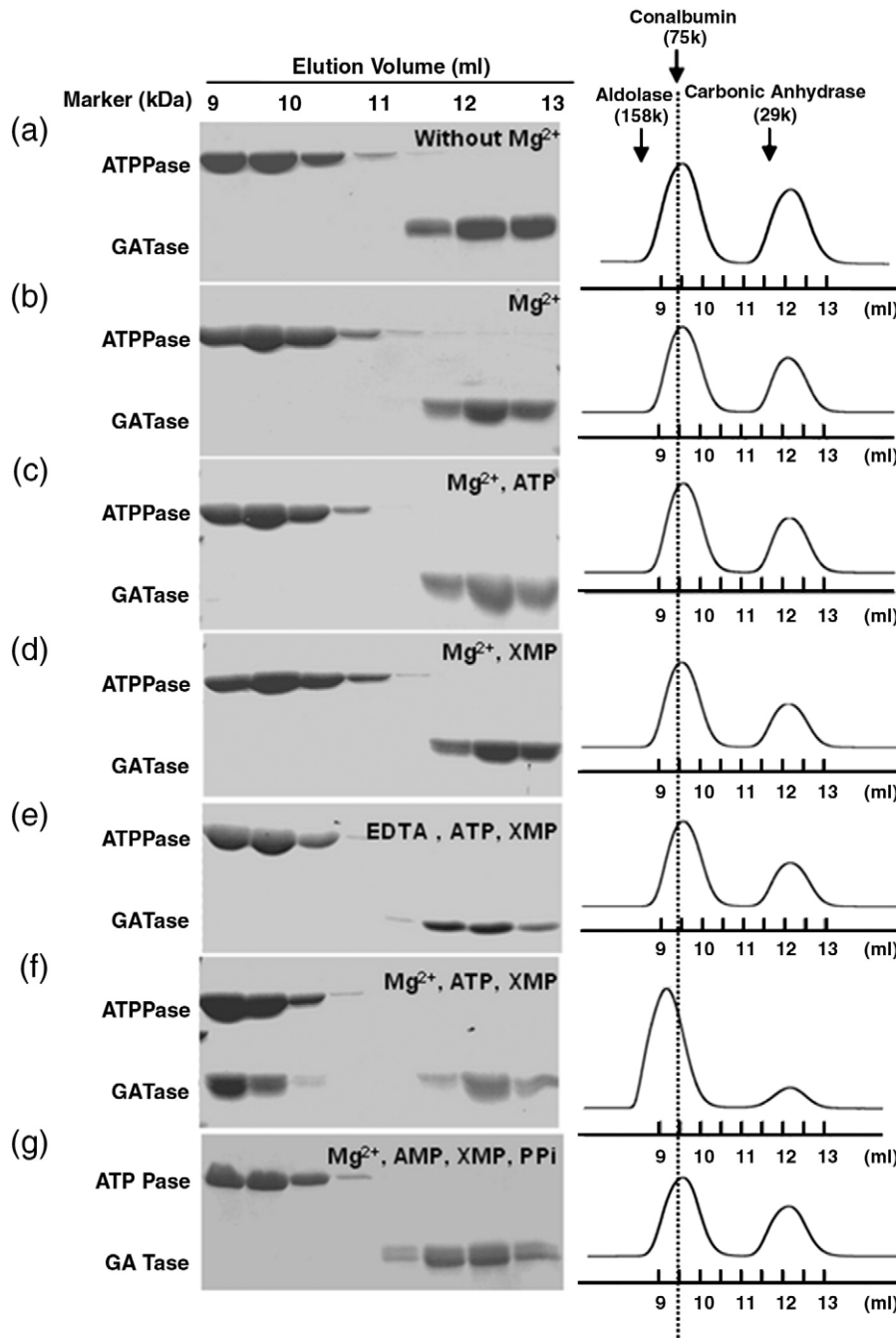


**Fig. 7.** Substrate-dependent complex formation of PH-ATPPase with PH-GATase. The reaction buffers used contained: no substrate (a); 10 mM MgCl<sub>2</sub> (b); 10 mM MgCl<sub>2</sub> and 0.1 mM ATP (c); 10 mM MgCl<sub>2</sub> and 0.1 mM XMP (d); 1 mM EDTA, 0.1 mM ATP, and 0.1 mM XMP (e); 10 mM MgCl<sub>2</sub>, 0.1 mM ATP, and 0.1 mM XMP (f); and 10 mM MgCl<sub>2</sub>, 0.1 mM AMP, 0.1 mM XMP, and PPI (g). The fractions obtained by gel-filtration chromatography with a Superdex 75 10/30 HR column were subjected to SDS-PAGE. PH-GATase (monomer) and PH-ATPPase (dimer) were eluted at elution volumes of 9.6 ml and 12.1 ml, respectively. Their complex was eluted at 9.2 ml. Aldolase (158k), conalbumin (75k), and carbonic anhydrase (29k) were used as markers.

grown in LB medium containing 30 µg/ml kanamycin at 310 K. Protein expression was induced with 1 mM IPTG. After 12 h, the cells were harvested by centrifugation at 5000g and resuspended in 20 mM Tris-HCl (pH 8.0). The cells were disrupted by sonication and centrifuged at 40,000g for 30 min. The supernatant was heated at 353 K for 30 min and centrifuged at 40,000g for 30 min. Then, 0.01% (final concentration) polyethyleneimine was added to the supernatant and stirred for 30 min on ice. After centrifu-

gation at 40,000g for 30 min, the supernatant was loaded onto a RESOURCE Q 6-ml column (GE Healthcare) equilibrated with 20 mM Tris-HCl (pH 8.0). The GMPS subunit was eluted at 80–100 mM NaCl in 20 mM Tris-HCl (pH 8.0). Then the fractions containing the GMPS subunit were pooled, concentrated, dialyzed against 20 mM Tris-HCl (pH 8.0) and 100 mM NaCl, and loaded onto a Superdex 75 10/30 column (GE Healthcare) equilibrated with 20 mM Tris-HCl (pH 8.0) and 100 mM NaCl. The

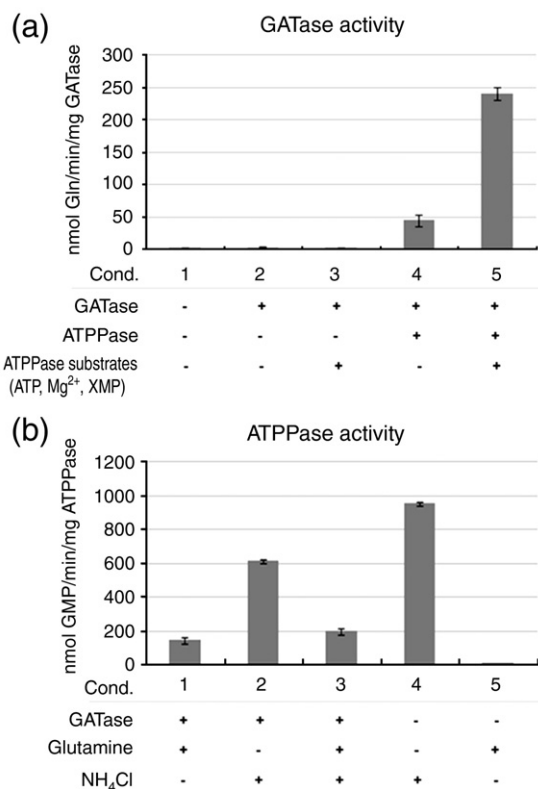


**Fig. 8.** Activity assays of PH-GATase and PH-ATPPase. (a) GATase activity was measured in a coupled enzymatic assay with GDH. The base reaction mixtures (Condition (1)) contained 60 mM Hepes buffer (pH 8.0), 0.8 mM EDTA, 20 mM Gln, 1 mM NADP<sup>+</sup>, and 10 nM GDH. A concentration of 1  $\mu$ M was used for the enzyme(s) (PH-GATase and/or PH-ATPPase), and the following concentrations were used for the ATPase substrates: 1 mM ATP, 0.3 mM XMP, and 20 mM MgCl<sub>2</sub>. (b) ATPase activity was measured using glutamine and ammonium chloride as donors of ammonia. The following concentrations were used: 2  $\mu$ M enzyme(s) (PH-ATPPase and/or PH-GATase) and 20 mM ammonia donor(s) (glutamine and/or ammonium chloride).

fractions containing the GMPS subunit were pooled, dialyzed against 5 mM Tris-HCl (pH 8.0), and concentrated to 30 mg/ml with a Centriprep-3 concentrator (Amicon). Purity was ascertained by SDS-PAGE, and concentration was determined by measuring absorbance at 280 nm with an extinction coefficient of 30,940 M<sup>-1</sup> cm<sup>-1</sup>.

### Crystallization and data collection of PH-ATPPase

Crystallization was performed at 278 K using sitting-drop vapor diffusion. Crystals of PH-ATPPase (0.4 mm  $\times$  0.3 mm  $\times$  0.1 mm) were obtained in 3 weeks by mixing 1  $\mu$ l of the protein solution and 1  $\mu$ l of the reservoir solution containing 30% (vol/vol) polyethylene glycol 400, 100 mM Tris-HCl (pH 8.4), and 200 mM MgCl<sub>2</sub>. A drop was equilibrated against 100  $\mu$ l of the reservoir solution. The crystals were flash-cooled to 100 K with a nitrogen cryostream. Diffraction data were collected at beamline NW12 of the Photon Factory Advanced Ring (Tsukuba, Japan). The diffraction data were indexed and scaled with HKL2000.<sup>28</sup> The crystal belonged to space group *P*2<sub>1</sub>2<sub>1</sub>2<sub>1</sub>

with unit cell dimensions  $a=69.9$  Å,  $b=82.2$  Å, and  $c=111.6$  Å, and an asymmetric unit contained two molecules of PH-ATPPase.

### Structure solution and refinement of PH-ATPPase

The structure of PH-ATPPase was determined by molecular replacement with the program MOLREP,<sup>29</sup> using the atomic coordinates of the ATPase domain of the GMPS from *E. coli* (PDB ID 1GPM) as initial model. Further model building was performed with the program Xfit,<sup>30</sup> and refinements were performed with XtalView<sup>30</sup> and Refmac5.<sup>31</sup> Solvent atoms were initially built using the program ARP/wARP<sup>32</sup> and later added or removed by manual inspection. The refined structure was validated with PROCHECK<sup>33</sup> and visualized with PyMOL<sup>‡</sup>.

### Expression and purification of PH-GATase for activity assay and gel-filtration analysis

PH-GATase was prepared as previously described,<sup>22</sup> with the following modifications. To obtain a tagless PH-GATase, we cloned the gene *ph1346* into pET26b (not pET28a) using the NdeI and BamHI sites. *E. coli* strain BL21(DE3) was used as the host for protein expression.

### Gel-filtration chromatography

To analyze the interaction of PH-ATPPase and PH-GATase, we performed gel-filtration chromatography under five buffer conditions. Each buffer contained 50 mM Tris-HCl (pH 8.0) and 100 mM NaCl, with the addition of the following substrates:

- buffer a: no substrate
- buffer b: 10 mM MgCl<sub>2</sub>
- buffer c: 10 mM MgCl<sub>2</sub> and 0.1 mM ATP
- buffer d: 10 mM MgCl<sub>2</sub> and 0.1 mM XMP
- buffer e: 1 mM ethylenediaminetetraacetic acid (EDTA), 0.1 mM ATP, and 0.1 mM XMP
- buffer f: 10 mM MgCl<sub>2</sub>, 0.1 mM ATP, and 0.1 mM XMP
- buffer g: 10 mM MgCl<sub>2</sub>, 0.1 mM AMP, 0.1 mM XMP, and 0.1 mM PPI

The mixture of 0.01 mM PH-GATase and 0.01 mM PH-ATPPase dissolved in five kinds of buffers was loaded onto a Superdex 75 10/30 column (GE Healthcare) at a flow rate of 0.5 ml/min at room temperature. The 0.5-ml fractions were collected and analyzed by 15% SDS-PAGE.

### GATase activity assay

The glutaminase activity of PH-GATase was measured in a coupled enzymatic assay with GDH (Wako, Japan). The glutamate produced by PH-GATase was oxidized by GDH in the presence of NADP<sup>+</sup>, yielding 2-oxoglutarate and NADPH+H<sup>+</sup>+NH<sub>3</sub>. The reaction was monitored by the increase in absorbance at 340 nm using the equation:  $\Delta\epsilon_{340} [\text{NADPH} - \text{NADP}^+] = 6220 \text{ M}^{-1} \text{ cm}^{-1}$ . The reaction mixtures contained 60 mM Hepes buffer (pH 8.0), 0.8 mM EDTA, 20 mM Gln, 1 mM NADP<sup>+</sup>, and 10 nM GDH. The substrates of PH-

‡ <http://pymol.sourceforge.net/>

ATPPase (1 mM ATP, 0.3 mM XMP, and 20 mM MgCl<sub>2</sub>) were either added or omitted from the reaction mixture. The enzyme(s), 1 μM PH-ATPPase, 1 μM PH-GATase, or both 1 μM PH-ATPPase and 1 μM PH-GATase (final concentration(s)) were added to start the reaction. All measurements were performed in triplicate.

### ATPPase activity assay

The assays for the ATPase activity were performed using glutamine and ammonium chloride as donors of ammonia, in accordance with a previously described method,<sup>26,34</sup> with some modifications. To a reaction mixture containing 2 μM PH-ATPPase, 2 μM PH-GATase, 60 mM Hepes buffer (pH 8.0), 1 mM ATP, 0.3 mM XMP, 20 mM MgCl<sub>2</sub>, 0.1 mM DTT, 0.8 mM EDTA, and the ammonia donor(s) (20 mM glutamine, 20 mM ammonium chloride, or both) were added to start the reaction. The reaction mixture was incubated at 323 K for 3 min. GMPs activity was monitored by a decrease in absorbance at 290 nm:  $\Delta\epsilon_{290} [\text{XMP} - (\text{GMP} + \text{AMP})] = 1500 \text{ M}^{-1} \text{ cm}^{-1}$ . To examine the effect of PH-GATase on the activity of PH-ATPPase, we also performed the assays without PH-GATase. All measurements were performed in triplicate.

### PDB accession number

Coordinates and structural factors for the structure of PH-ATPPase have been deposited with the Research Collaboratory for Structural Bioinformatics PDB with accession code 3A4I.

### Acknowledgements

We thank the beamline staff at the Photon Factory for their kind help with data collection. Synchrotron radiation experiments were performed with the approval of the Photon Factory, KEK (2003G130, 2003S2-002, and 2008S2-001). This work was supported, in part, by grants from the National Project on Protein Structural and Functional Analyses of the Ministry of Education, Culture, Sports, Science, and Technology of Japan; the Targeted Proteins Research Program; and Grants-in-Aid for Scientific Research from the Ministry of Education, Culture, Sports, Science, and Technology of Japan.

### Supplementary Data

Supplementary data associated with this article can be found, in the online version, at [doi:10.1016/j.jmb.2009.10.053](https://doi.org/10.1016/j.jmb.2009.10.053)

### References

- Knaap, J. A., Kumar, B. R., Moshkin, Y. M., Langenberg, K., Krijgsveld, J., Heck, A. J. *et al.* (2005). GMP synthetase stimulates histone H2B deubiquitylation by the epigenetic silencer USP7. *Mol. Cell*, **17**, 695–707.
- Long, H., Cameron, S., Yu, L. & Rao, Y. (2006). *De novo* GMP synthesis is required for axon guidance in *Drosophila*. *Genetics*, **172**, 1633–1642.
- Ishikawa, H. (1999). Mizoribine and mycophenolate mofetil. *Curr. Med. Chem.* **6**, 575–597.
- Lagerkvist, U. (1958). Biosynthesis of guanosine 5'-phosphate. *J. Biol. Chem.* **233**, 143–149.
- Fukuyama, T. & Moyed, H. S. (1964). A separate antibiotic-binding site in xanthosine-5'-phosphate aminase: inhibitor- and substrate-binding studies. *Biochemistry*, **3**, 1488–1492.
- von der Saal, W., Crysler, C. S. & Villafranca, J. J. (1985). Positional isotope exchange and kinetic experiments with *Escherichia coli* guanosine-5'-monophosphate synthetase. *Biochemistry*, **24**, 5343–5350.
- Raushel, F. M., Thoden, J. B. & Holden, H. M. (1999). The amidotransferase family of enzymes: molecular machines for the production and delivery of ammonia. *Biochemistry*, **38**, 7891–7899.
- Zalkin, H. & Smith, J. L. (1998). Enzymes utilizing glutamine as an amide donor. *Adv. Enzymol. Relat. Areas Mol. Biol.* **72**, 87–144.
- Thompson, J. D., Higgins, D. G. & Gibson, T. J. (1994). CLUSTAL W: improving the sensitivity of progressive multiple sequence alignment through sequence weighting, position-specific gap penalties and weight matrix choice. *Nucleic Acids Res.* **22**, 4673–4680.
- Gouet, P., Courcelle, E., Stuart, D. I. & Métoz, F. (1999). ESPript: analysis of multiple sequence alignments in PostScript. *Bioinformatics*, **15**, 305–308.
- Lou, L., Nakamura, J., Tsing, S., Nguyen, B., Chow, J., Straub, K. *et al.* (1995). High-level production from a baculovirus expression system and biochemical characterization of human GMP synthetase. *Protein Expression Purif.* **6**, 487–495.
- Nakamura, J. & Lou, L. (1995). Biochemical characterization of human GMP synthetase. *J. Biol. Chem.* **270**, 7347–7353.
- Nakamura, J., Straub, K., Wu, J. & Lou, L. (1995). The glutamine hydrolysis function of human GMP synthetase. Identification of an essential active site cysteine. *J. Biol. Chem.* **270**, 23450–23455.
- Hirai, K., Matsuda, Y. & Nakagawa, H. (1987). Purification and characterization of GMP synthetase from Yoshida sarcoma ascites cells. *J. Biochem.* **102**, 893–902.
- Spector, T. (1975). Studies with GMP synthetase from Ehrlich ascites cells. Purification, properties, and interactions with nucleotide analogs. *J. Biol. Chem.* **250**, 7372–7376.
- Sakamoto, N., Hatfield, G. W. & Moyed, H. S. (1972). Physical properties and subunit structure of xanthosine 5'-phosphate aminase. *J. Biol. Chem.* **247**, 5880–5887.
- Patel, N., Moyed, H. S. & Kane, J. F. (1975). Xanthosine-5'-phosphate amidotransferase from *Escherichia coli*. *J. Biol. Chem.* **250**, 2609–2613.
- Deras, M. L., Chittur, S. V. & Davisson, V. J. (1999). N<sup>2</sup>-Hydroxyguanosine 5'-monophosphate is a time-dependent inhibitor of *Escherichia coli* guanosine monophosphate synthetase. *Biochemistry*, **38**, 303–310.
- Chittur, S., Klem, T., Shafer, C. & Davisson, V. (2001). Mechanism for acivicin inactivation of triad glutamine amidotransferases. *Biochemistry*, **40**, 876–887.
- Bhat, J. Y., Shastri, B. G. & Balaram, H. (2008). Kinetic and biochemical characterization of *Plasmodium falciparum* GMP synthetase. *Biochem. J.* **409**, 263–273.

21. Tesmer, J. J., Klem, T. J., Deras, M. L., Davisson, V. J. & Smith, J. L. (1996). The crystal structure of GMP synthetase reveals a novel catalytic triad and is a structural paradigm for two enzyme families. *Nat. Struct. Biol.* **3**, 74–86.
22. Maruoka, S., Lee, W. C., Kamo, M., Kudo, N., Nagata, K. & Tanokura, M. (2005). Crystal structure of glutamine amidotransferase from *Pyrococcus horikoshii* OT3. *Proc. Jpn. Acad.* **81**, 459–462.
23. Krissinel, E. & Henrick, K. (2007). Inference of macromolecular assemblies from crystalline state. *J. Mol. Biol.* **372**, 774–797.
24. Tesmer, J. J., Stemmler, T. L., Penner-Hahn, J. E., Davisson, V. J. & Smith, J. L. (1994). Preliminary X-ray structure of GMP synthetase: determination of anomalous scattering factors for a cysteinyl mercury derivative. *Proteins*, **18**, 394–403.
25. Zalkin, H. & Truitt, C. (1977). Characterization of the glutamine site of *Escherichia coli* guanosine 5'-monophosphate synthetase. *J. Biol. Chem.* **252**, 5431–5436.
26. Zalkin, H. (1985). Glutamine amidotransferases. *Methods Enzymol.* **113**, 263–264.
27. Matte-Tailliez, O., Brochier, C., Forterre, P. & Philippe, H. (2002). Archaeal phylogeny based on ribosomal proteins. *Mol. Biol. Evol.* **19**, 631–639.
28. Otwinowski, Z. & Minor, W. (1997). Processing of X-ray diffraction data collected in oscillation mode. *Methods Enzymol.* **276**, 307–326.
29. Vagin, A. & Teplyakov, A. (1997). MOLREP: an automated program for molecular replacement. *J. Appl. Crystallogr.* **30**, 1022–1025.
30. McRee, D. E. (1999). XtalView/Xfit—a versatile program for manipulating atomic coordinates and electron density. *J. Struct. Biol.* **125**, 156–165.
31. Murshudov, G. N., Vagin, A. A. & Dodson, E. J. (1997). Refinement of macromolecular structures by the maximum-likelihood method. *Acta Crystallogr. Sect. D*, **53**, 240–255.
32. Perrakis, A., Morris, R. & Lamzin, V. S. (1999). Automated protein model building combined with iterative structure refinement. *Nat. Struct. Biol.* **6**, 458–463.
33. Laskowski, R. A., MacArthur, M. W., Moss, D. S. & Thornton, J. M. (1993). PROCHECK: a program to check the stereochemical quality of protein structures. *J. Appl. Crystallogr.* **26**, 283–291.
34. Abbott, J., Newell, J., Lightcap, C., Olanich, M., Loughlin, D., Weller, M. *et al.* (2006). The effects of removing the GAT domain from *E. coli* GMP synthetase. *Protein J.* **25**, 483–491.